

Available online on 18.08.2019 at <http://jddtonline.info>

Journal of Drug Delivery and Therapeutics

Open Access to Pharmaceutical and Medical Research

© 2011-18, publisher and licensee JDDT, This is an Open Access article which permits unrestricted non-commercial use, provided the original work is properly cited

Open  Access

Research Article

Studies on solvent systems for enhanced skin permeation of venlafaxine hydrochloride

Pramod S. Salve*, Shahadev B. Rathod

University Department of Pharmaceutical Sciences, Rashtrasant Tukadoji Maharaj Nagpur University Campus, Mahatma Jyotiba Fuley Shaikshanik Parisar Amravati Road, Nagpur -440 033 (M.S.)

ABSTRACT

Venlafaxine hydrochloride (VH) is a serotonin-noradrenaline reuptake inhibitor indicated for treatment of depression disorder. It shows low biological half-life 5 ± 2 h and low oral bioavailability 45 ± 15 % due to extensive hepatic first-pass metabolism. Frequent administration of VH is required to maintain steady state plasma concentration of drug. To overcome hepatic first pass metabolism and to cross blood brain barrier for effectively achieving plasma concentration of VH in brain, we envisaged to develop transdermal drug delivery system containing VH loaded polymeric nanoparticles. Effect of solvent systems (SS), penetration enhancers (PE), and VH nanoparticles (VHNPs) on transdermal diffusion of drug were studied. VHNPs were prepared by double emulsion solvent evaporation method using high speed homogenizer followed by probe sonication. Poly (lactic-co-glycolic acid) and tween 80 were used as polymer and surfactant respectively. Mean particle size, polydispersity index, zeta potential, entrapment efficiency of optimized VHNPs were found to be 175.4 nm, 0.109, (-) 24 mV and 56 % respectively. Scanning electron microscopy confirmed spherical shape of drug loaded polymeric nanoparticles. SS comprising 50% PG in EtOH shown maximum flux 158.67 ± 2.9 ($\mu\text{g}/\text{cm}^2/\text{h}$) and lag time was found to be 5.60 ± 0.16 h. The PE 5 (%v/v) limonene shown maximum flux 200.47 ± 3.6 ($\mu\text{g}/\text{cm}^2/\text{h}$) and lag time 3.17 ± 0.11 h. The flux and lag time in case of VHNPs were found to be 192.24 ± 3.20 ($\mu\text{g}/\text{cm}^2/\text{h}$) and 4.22 ± 0.14 h respectively. Based on flux, clearance and surface area of transdermal patch, a theoretical meaningful plasma level concentration of VH ranging from 12.85 to 128.5 (ng/mL) can be achieved.

Keywords: Depression, Venlafaxine hydrochloride, Poly (lactic-co-glycolic acid), Solvent systems, Penetration enhancers, Nanoparticles (NPs)

Article Info: Received 09 June 2019; Review Completed 26 July 2019; Accepted 06 Aug 2019; Available online 18 August 2019



Cite this article as:

Salve PS, Rathod SB, Studies on solvent systems for enhanced skin permeation of venlafaxine hydrochloride, Journal of Drug Delivery and Therapeutics. 2019; 9(4-s):505-518 <http://dx.doi.org/10.22270/jddt.v9i4-s.3379>

*Address for Correspondence:

Pramod S. Salve, University Department of Pharmaceutical Sciences, Rashtrasant Tukadoji Maharaj Nagpur University Campus, Mahatma Jyotiba Fuley Shaikshanik Parisar Amravati Road, Nagpur -440 033 (M.S.)

INTRODUCTION

Depression is major psychological condition disturbing 340 million people worldwide. Present data shows that 9% children by age 14 have previously experienced a minimum one episode of severe depression, while up to 10% of young people are affected by a major depressive disorder [Dinas P. *et al.* 2011].

The change in the levels of monoamines serotonin, norepinephrine (NE) and dopamine (DA) results in depression. VH is a serotonin-noradrenaline reuptake inhibitor, indicated for the treatment of depression [Zhou Y. *et al.* 2015]. Serotonin noradrenaline reuptake inhibitors increase the levels of serotonin and noradrenaline in brain by blocking their reuptake by nerves. The patients suffering from depression shows lowered mood, abstinence from pleasure, disturbed food habits, feelings of sorrow, lack of concentration in doing things. These problems culminate

into disability or development of suicidal tendencies [Dinas P. *et al.* 2011].

Central nervous system (CNS) shows barrier property for drug penetration in brain. Blood brain barrier (BBB) and blood cerebrospinal fluid barrier (BCSFB) restricts entry of drug in brain [Abbott N 2010]. It is observed that nearly 100% of large molecules and 98% of small molecules does not cross BBB [Tosi G *et al.* 2008, Bellavance M. 2010]. To overcome these difficulties, use of biocompatible drug-loaded polymeric nanoparticles (PNPs) has been proposed [Alexis *et al.* 2008].

VH is a highly water soluble, non-tricyclic antidepressant drug. It is serotonin-norepinephrine reuptake inhibitor. It involves 5HT_{1a}, 5HT_{1b} and 5HT_{2a} receptors. VH is 5-HT-dopamine activity modulator, dopamine D₂ partial agonist and used in treatment of major depressive disorder [Barch D. 2013]. The steady state biological half-lives of venlafaxine

and its active metabolite o-desmethylvenlafaxine are 5 and 11 h respectively [Gohel M. 2009].

The low biological half-life 5 ± 2 hours coupled with low oral bioavailability $45 \pm 15\%$ due to its extensive first-pass metabolism requires frequent drug administration to maintain effective plasma concentration of VH. The immediate-release oral formulations have side-effects, including nausea, insomnia, weakness, drowsiness and constipation [Patel H. *et al.* 2011].

Drugs used in the treatment of depression are selective serotonin reuptake inhibitors, tricyclic antidepressants, monoamine oxidase inhibitors, serotonin norepinephrine reuptake inhibitors [Tripathi K.D. *et al.* 2009].

Polymeric nanoparticles (PNPs) are solid, colloidal particles prepared from biocompatible and biodegradable polymers in size between 10-1000 nm where the drug is dissolved, entrapped, encapsulated or attached to a nanoparticle matrix. Depending upon the method of preparation, nanospheres or nanocapsules can be obtained [Anderson J. and Shive M. 1977]. Nanocapsules are systems in which the drug is confined to a cavity surrounded by a unique polymer membrane, while nanospheres are matrix systems in which the drug is physically and uniformly dispersed.

PLGA is a widely used polymer for development of nanoparticles because of biocompatibility and potential to cross the blood brain barrier. [Acharya S. and Sahoo S., 2011]. The polymer has been intensively utilized for drug delivery and to encapsulate both water-soluble and water-insoluble drugs [Danhier F. *et al.* 2012].

To overcome the hepatic first pass metabolism of VH, it was envisaged to develop transdermal drug delivery system containing VH loaded polymeric nanoparticles.

Selection of suitable solvent system is the important step in the development of transdermal drug delivery systems. Solvent systems comprising ethanol, propylene glycol and their binary combinations with water in various proportions were studied. The effect of penetration enhancers were studied for their effect on *ex-vivo* skin permeation of VH [Panchagnula R *et al.* 2001]. It was envisaged to compare the lag time, and flux values of VH, VHNPs with the solvent systems studied in the *ex-vivo* skin permeation studies.

MATERIALS AND METHOD

Materials

VH was obtained as a gratis sample from Amoli Organics Pvt. Ltd. Mumbai, India. Poly (lactic co-glycolic acid) 50:50 (Molecular weight.24000-38000 Da) was obtained as a gratis sample from Evonik India Pvt. Ltd. Mumbai, India. Tween 80 was obtained from Loba Chemie Pvt. Ltd, India. Ethylene vinyl acetate copolymer (EVAC), dibutyl phthalate, ethanol, propylene glycol, cineole, limonene, and menthol were procured from Merck India Pvt. Ltd, India. Purified water was obtained from Milli-Q water purification system.

Method

Preparation of polymeric nanoparticles of VH

Polymeric nanoparticles of VH with PLGA polymer were prepared by double emulsion solvent evaporation method. The drug, VH was dissolved in distilled water and poly(lactic co-glycolic acid) was dissolved in dichloromethane. A w/o type emulsion was prepared using various concentrations of drug: polymer ratio (Table 1). An accurately weighed amount of VH and PLGA polymer were dissolved in 2 mL distilled water and 6 mL dichloromethane respectively to form w/o type primary emulsion [Bilati U. *et al.* 2005, Vandervoort J. *et al.* 2002].

The primary emulsion was dropwise added using syringe into aqueous phase (w) containing tween-80 surfactant solutions. The resulting w/o/w type secondary formed was kept overnight on continuous magnetic stirring at room temperature for complete evaporation of dichloromethane. The secondary emulsion was homogenized using a high-speed homogenizer (IKA Ultra Turrex T18, Germany) at 12,000 rpm speed for 15 min followed by probe sonication (Sonic Vibra Cell™) at 80 % amplitude for 10 min.

The polymeric nanoparticles were recovered by centrifugation using a refrigerated centrifuge at 20,000 rpm for 1 hour at 4 °C. The supernatant liquids were discarded and washed thrice with distilled water to remove the adsorbed polymer and drug. The pellets formed of nanoparticles was obtained after centrifugation (Remi C24 Plus). To the formed pellet, a 5 (%w/v) solution of mannitol was added as cryoprotectant and filled in glass vials. The vials were freeze dried at (-) 40 °C and 750 mm/Hg vacuum pressure out for 72 h. The freeze-dried powder product was stored in refrigerator in airtight glass container.

Table 1 Formulation of VH loaded polymeric PLGA nanoparticles

Formulation code	Dose of drug (VH)	Solvents Water: DCM in 1:3 ratio	Factor 1	Factor 2	Distilled water (q.s.)
			A: Concentration of PLGA polymer	B:Concentration of surfactant tween-80	
	mg	mL	mg	%v/v	mL
F1	37.5	2	37.5	2.0	100
F2	37.5	2	37.5	0.5	100
F3	37.5	2	75	2.0	100
F4	37.5	2	75	1.0	100
F5	37.5	2	75	0.5	100
F6	37.5	2	112.5	0.5	100
F7	37.5	2	37.5	1.0	100
F8	37.5	2	112.5	1.0	100
F9	37.5	2	112.5	2.0	100

Experimental Design

A full factorial design for two factors at three levels each was selected to optimize response of variables. The two factors, PLGA sustained release polymer (mg) and tween 80 (%v/v) used were varied and the factor levels were suitably coded. The particle size, polydispersity index, zeta potential and % entrapment efficiency were taken as the response variables. In the design, the two factors were evaluated each at three levels and experimental trials were performed for possible combinations. All other formulation variables and processing variables were kept constant throughout the studies.

The formulae were developed as 9 sets varying the variables following 3^2 full factorial design (3 levels) using Design expert software. Dependent variables were Y1 = Particle size Y2 = Polydispersity index, Y3= Zeta potential and Y4=% Entrapment efficiency. The effect of two independent variables PLGA (X1) and Tween-80 (X2) on the responses (Y1, Y2, Y3 and Y4) were observed. The levels of all other ingredients in the formulation were fixed.

Characterization of lyophilized VH loaded polymeric PLGA Nanoparticles

Determination of particle size, polydispersity index (PDI) and zeta potential

Lyophilized dried powders of nanoparticles were dispersed in distilled water and were kept in an ultrasonicator for 40

seconds. The mean particle size (z average), zeta potential, and polydispersity index (PDI) of aqueous dispersion of VH loaded PPNPs were measured by a dynamic light scattering method using a Zetasizer Nano ZS-90 (Malvern Instruments, Worcestershire, UK). Each value recited was the average of determinations on three independent samples of different batches of each formulation. If PDI value is closer to 0, it indicates narrow size distribution of the particles. PDI of optimized dispersion was below 0.5 which indicated prepared dispersion is monodisperse and will remain stable [Katara R. *et.al.* 2017].

Determination of percent entrapment efficiency and percent drug loading

VH loaded NPs and naive NPs were obtained as pellets after centrifugation at 18000 rpm for 60 min at 4 °C. The absorbance of the clear supernatant obtained after centrifugation of dispersion of drug loaded NPs was analyzed in UV spectrophotometer (SHIMADZU 1800) at λ_{max} 226 nm against the supernatant obtained from the dispersion of naive NPs and was used as blank. The clear supernatant also contained the free drug which was obtained by washing of the NPs, in the dispersion with deionized water.

The drug entrapment efficiency was determined using the equation 1 [Lopez E. *et al.*, 2016].

$$\%EE = \frac{\text{Total amount of VH added} - \text{Free VH in supernatant liquid}}{\text{Total amount of VH added}} \times 100 \quad \text{----- (1)}$$

Polymer drug interaction studies of lyophilized nanoparticles

The polymer drug interaction studies of lyophilized nanoparticles were performed using FT-IR spectroscopy, differential scanning calorimetry and x-ray diffraction spectroscopy and scanning electron microscopy studies.

FT-IR spectroscopy

FT-IR spectrum of VH, PLGA polymer and optimized formulation F9 was measured in solid state as potassium bromide mixture. (FTIR 8300 Shimadzu, Tokyo, Japan). The samples were previously ground and mixed thoroughly with potassium bromide, an infrared transparent matrix at 1:100 (Sample: KBr) ratio, respectively. The spectrum was recorded in the range 4000–400 cm^{-1} [Katara R. *et.al.* 2017].

Differential scanning calorimetry (DSC)

The sample of VH, PLGA polymer and lyophilized nanoparticles of optimized formulation F9 was kept in desiccator for 24 h before thermal analysis. An accurately weighed sample, 5 mg was hermetically sealed in aluminium crucible and DSC analysis was performed using DSC TA-60 (Shimadzu, Tokyo, Japan) calorimeter heated at constant rate of 10 °C/min. over a temperature range 40 to 400 °C. An inert atmosphere was maintained by purging nitrogen gas at a flow rate of 50 mL/min. An empty aluminium pan was used as a reference [Katara R. *et.al.* 2017].

X-ray diffraction (X-RD) spectroscopy

X-ray diffraction spectrum of VH, PLGA and lyophilized nanoparticles of optimized formulation F9 was recorded in diffractometer (Rigaker Geigerflex, Japan) using Cu-K α line as source of radiation at a voltage of 35 Kv and current 25 mA. The sample was measured in an angle 2 θ range between 3-80 ° and 0.0053 step size [Katara R. *et al.* 2017, Sawant *et al.* 2011].

Scanning electron microscopic (SEM) study

Shape and surface morphology of VH PPNPs was visualized by scanning electron microscopy (LEO-430 Cambridge and U.K). Samples were prepared by lightly sprinkling nanoparticles on a double adhesive tape on an aluminum stub. The stubs were coated with gold to a thickness of 200 to 500 Å under an argon atmosphere using gold sputter module in a high vacuum evaporator. The samples were then randomly scanned and photomicrographs were recorded at different magnifications with SEM [Gulati N. *et al.* 2014].

Ex-vivo skin permeation studies

For preparation of whole skin, the animal was sacrificed by excess inhalation of diethyl ether anesthetic agent. The abdominal skin of animal was shaved with the help of animal hair remover or clipper in the direction of tail to head without causing damage to skin. The shaved skin was excised with the help of surgical blade (size 24) fitted in a surgical blade holder (size 4). The adhered tissues to the dermis were removed with the help of cotton swab moistened with isopropyl alcohol. The skin was washed with distilled water, wrapped in aluminum foil and stored in freezer at (-) 20 °C until further use. The skin was thawed to room temperature.

It was kept in thermostatic shaker bath at 37 ± 1 °C temperature for 1 h. The receptor fluid phosphate buffer pH 7.4 containing 0.01% sodium azide was added in the receptor medium to retard microbial growth and equilibrated to bring it to 37 ± 1 °C temperature [Panchagnula R. *et al.* 2001].

The skin was cut into circular pieces to a size of external circumference of donor compartment and mounted on diffusion cell assembly, keeping stratum corneum side towards donor compartment and equilibrated for 1 h. Depending on drug solubility of VH, the binary combination of ethanol, propylene glycol and their binary combinations with water in various proportions were used as solvent system for *ex-vivo* skin permeation studies as shown in table 2. In the 2 mL solvent system, 37.5 mg was dissolved and added in donor phase compartment of diffusion assembly. Based on the flux values, optimized solvent system was

selected showing highest flux as compared to other binary solvent systems studied. The effect of penetration enhancer, cineole, limonene, menthol were studied by incorporating them individually in the optimized binary combination of solvent system used in *ex-vivo* permeation studies. From the receptor compartment, 1 mL volume was withdrawn at 0, 1, 2, 4, 6, 8, 10, 12, 16, 20, 24, 36 and 48 h and replaced with equal volume of fresh receptor phase every time to determine the amount of drug permeated through the skin.

Cartesian plots were made taking time in hours on x-axis and cumulative amount of drug permeated in receptor fluid on y-axis. The lag time, flux, permeability, and enhancement ratio were calculated. Flux values ($\mu\text{g}/\text{cm}^2/\text{h}$) were calculated from the slopes of the steady states of above plots. Lag times were calculated from the intercepts of extrapolated steady state flux to x-axis. Flux, Permeability coefficient and enhancement ratio were calculated using equation 2.

- A) The flux (J_{ss}) ($\text{mg}/\text{cm}^2/\text{h}$) was calculated from the slope of the plot of the cumulative amount of drug permeated per cm^2 of skin at steady state against time using linear regression analysis.

$$J_{ss} = (dy/dx)_{ss} \times 1/A \quad \text{----- (2)}$$

Where, $(dy/dx)_{ss}$ = Steady state slope and

A = Effective diffusion area

- B) Permeability coefficient (P) were determined by using equation 3 [Krishnaiah Y.2008].

$$\text{Permeability (P)} = \frac{\text{Steady State Flux (J)}}{\text{Concentration of drug in donor solution (C)}} \quad \text{----- (3)}$$

- C) Enhancement ratio (ER) were determined by using following equation [Krishnaiah Y.2008].

$$\text{Enhancement ratio (ER)} = \frac{\text{Flux of drug with penetration enhancer}}{\text{Flux of drug without penetration enhancer}} \quad \text{----- (4)}$$

Table 2 Solvent systems, permeation enhancers for *ex-vivo* skin permeation studies of VH and polymeric nanoparticles of VH

Sr. No.	FC	Solvent system	Dose of VH (mg)	PG (mL)	EtoH (mL)	DW (mL)	PPNPs VH (mL)	PE (%)
1	W	Water (Control)	37.5			2.0		
2	NPs	Nanoparticles	37.5				2.0	
3	V1	33% EtoH in DW	37.5		0.7	1.3		
4	V2	50% EtoH in DW	37.5		1.0	1.0		
5	V3	66% EtoH in DW	37.5		1.3	0.7		
6	V4	100 % EtoH	37.5		2.0			
7	V5	33% PG in DW	37.5	0.7		1.3		
8	V6	50% PG in DW	37.5	1.0		1.0		
9	V7	66% PG in DW	37.5	1.3		0.7		
10	V8	100% PG	37.5	2.0				
11	V9	33% PG in EtoH	37.5	0.7	1.3			
12	V10	50% PG in EtoH	37.5	1.0	1.0			
13	V11	66% PG in EtoH	37.5	1.3	0.7			
14	V12	5% Cineole (50% PG in EtoH)	37.5					5%
15	V13	5% Limonene (50% PG in EtoH)	37.5					5%
16	V14	5% Menthol (50% PG in EtoH)	37.5					5%

FC- Formulation code, VH- venlafaxine hydrochloride, PG- propylene glycol, EtoH- Ethanol, DW- Distilled water, PPNPs VH- polymeric PLGA nanoparticles comprising VH, PE- Permeation enhancers

RESULTS AND DISCUSSION

Experimental design

The formulations were prepared as 9 sets using two variables following 3^2 factorial designs. VH loaded polymeric PLGA NPs were prepared by double emulsion solvent

evaporation technique. The optimized formulations selected by the design were prepared and the parameters were compared to the expected values. The results are shown in table 3. For systematic investigation of the factors, a full factorial design was employed.

Table 3 Optimization of formulation by using 3^2 full factorial design

Formulation code	Dose of VH	Solvents DW: DCM (1:3)ratio	Factor 1	Factor 2	Response 1	Response 2	Response 3	Response 4
			A: Concentration of PLGA polymer	B: Concentration of Tween-80 surfactant	Particle size	PDI	Zeta potential	Entrapment efficiency
	mg	mL	mg	%v/v	nm	-	mV	%
F1	37.5	2	37.5	2.0	128.4 ±2.25	0.181 ±0.05	-6.8 ±0.26	36 ±3.12
F2	37.5	2	37.5	0.5	78.2 ±1.96	0.103 ±0.03	-12.4 ±0.41	33 ±1.95
F3	37.5	2	75	2.0	214.6 ±3.22	0.331 ±0.07	-15.2 ±0.32	45 ±3.05
F4	37.5	2	75	1.0	188.1 ±2.86	0.276 ±0.06	-14.3 ±0.54	43 ±2.68
F5	37.5	2	75	0.5	163.8 ±2.94	0.243 ±0.03	-12.7 ±0.37	40 ±2.08
F6	37.5	2	112.5	0.5	192.6 ±3.18	0.291 ±0.09	-10.2 ±0.30	47 ±1.12
F7	37.5	2	37.5	1.0	97.6 ±1.37	0.137 ±0.05	-9.8 ±0.62	31 ±1.98
F8	37.5	2	112.5	1.0	201.3 ±3.42	0.238 ±0.08	-10.5 ±0.29	51 ±2.14
F9	37.5	2	112.5	2.0	175.4 ±1.48	0.109 ±0.06	-24.0 ±0.33	56 ±3.56

Data were expressed as mean ± SD (n=3)

The effect on particle size (Y1) was observed to be significant by ANOVA and the polynomial equation was found to follow equation 5.

$$Y_1 = 218.586 + 42.1048 * A + 11.8881 * B - 18.7071 * AB - 65.225 * A^2 - 9.175 * B^2 \quad \text{----- (5)}$$

The terms A and B indicate concentrations of polymers PLGA and tween 80 respectively. As shown in equation 5, the positive sign with terms A and B indicated directly proportional relationship between concentration of polymers and particles size. As the concentrations of both polymers and surfactant were increased, the particles size was found to be increased. For response Y1 as shown in table 4, the coefficient of determination value (R^2) was found to be 0.9880 indicating a good fit agreement between concentrations of polymers and particle size. The 3D surface response plot of particle size and its contour plot are shown in figure 1 (A) and (B) respectively.

The effect on polydispersity index (Y2) was observed to be significant by ANOVA and the polynomial equation was found to follow equation 6.

$$Y_2 = 0.314189 + 0.0283656 * A - 0.0104677 * B - 0.0702092 * AB - 0.13375 * A^2 - 0.00725 * B^2 \quad \text{----- (6)}$$

The term A indicates concentration of PLGA whereas, term B indicates concentration of tween 80. By analyzing the equation, the positive response was observed for polydispersity index with PLGA. In case of tween 80, a negative response indicating the decreased polydispersity index was observed with decreased in tween 80 concentration. The coefficient of determination was found to be value (R^2) 0.9424 indicated the best fit agreement between effect of polymers on polydispersity index. The 3D surface response plot of polydispersity index and its contour plot are shown in figures 1 (C) and (D) respectively.

The effect on zeta potential (Y3) was observed to be significant by ANOVA and the polynomial equation was found to follow equation 7.

$$Y_3 = -14.4046 - 3.17049 * A - 2.33716 * B - 4.98444 * AB + 2.9875 * A^2 - 1.6 * B^2 \quad \text{----- (7)}$$

The term A indicates concentration of PLGA whereas term B indicates concentration of tween 80. By analyzing the equation, a negative response was observed for zeta potential with increasing concentration of tween 80 and PLGA. The coefficient of determination (R^2) was found to be 0.9524 indicating the good fit agreement between effects of polymers on particle size, PDI, zeta potential and entrapment efficiency. The 3D surface response plot of particle size, PDI, zeta potential and entrapment efficiency and its contour plot are shown in figures 1 (E) and (F) respectively.

The effect on entrapment efficiency (Y4) was observed to be significant by ANOVA and the polynomial equation was found to follow equation 8.

$$Y_4 = 46.2385 + 9.14668 * A + 2.98002 * B + 1.32015 * AB - 3.75 * A^2 + 0.25 * B^2 \quad \text{----- (8)}$$

The term A indicates concentration of PLGA whereas term B indicates concentration of tween 80. By analysing the equation, polymer and surfactant concentration were found to increase entrapment efficiency. The coefficient of determination (R^2) was found to be 0.9614 indicating the good fit agreement between effects of polymers on particle size, PDI, zeta potential and entrapment efficiency. The 3D surface response plot of particle size, PDI, zeta potential and entrapment efficiency and its contour plot are shown in figures 1 (G) and (H) respectively.

The p-values for particle size, PDI, Zeta potential and entrapment efficiency were found to be 0.004, 0.04 and 0.03 and 0.005 respectively. Thus, the P-values were found to be significant.

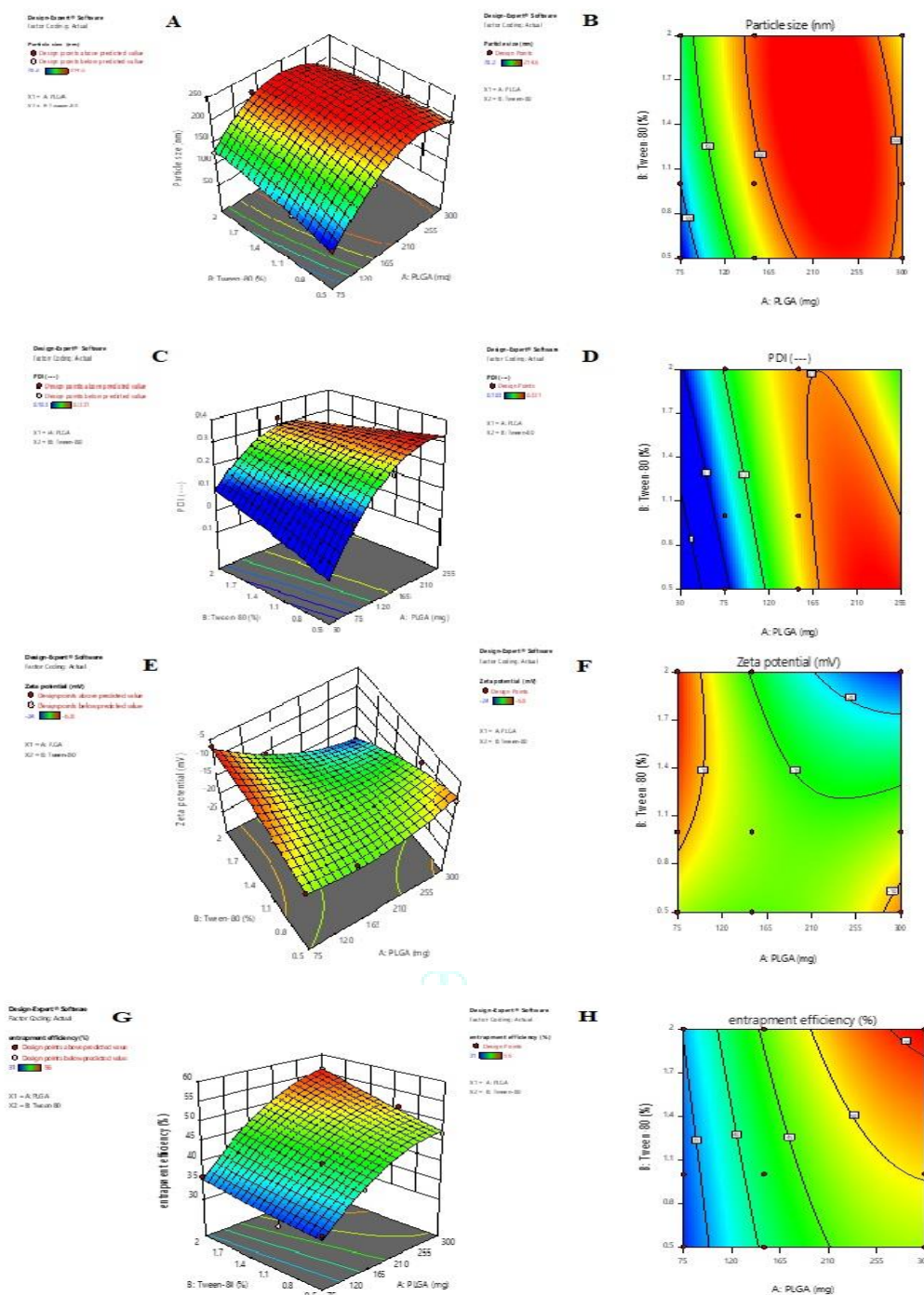


Fig. 1 3D response surface plot and contour plot of particle size, PDI, zeta potential and % EE of VH loaded PNPs

(A) 3D response surface plot of particle size VH loaded PNPs (B) Contour plot of particle size VH loaded PNPs (C) 3D response surface plot of PDI VH loaded PNPs (D) Contour plot of PDI VH loaded PNPs (E) 3D response surface plot of zeta potential VH loaded PNPs (F) Contour plot of zeta potential VH loaded PNPs (G) 3D response surface plot of % EE VH loaded PNPs (H) Contour plot of %EE VH loaded PNPs

Characterization of VH loaded PNPs

Determination of particle size, polydispersity index (PDI) and zeta potential

The particle size and PDI of the VH loaded polymeric PLGA nanoparticles are important characters in determining the capability of the particles to cross the BBB. The particle size and PDI of formulations (F1-F9) were obtained using Zetasizer Nano ZS 90 and the results are depicted in table 4

and particle size and PDI of optimized formulation F9 is shown in Fig. 2.

Table 4 Evaluations of particle size and PDI of formulations F1-F9

Sr. No.	Formulations	Particle Size (nm)	PDI
1	F1	128.4 ± 2.25	0.181 ± 0.05
2	F2	78.2 ± 1.96	0.103 ± 0.03
3	F3	214.6 ± 3.22	0.331 ± 0.07
4	F4	188.1 ± 2.86	0.276 ± 0.06
5	F5	163.8 ± 2.94	0.243 ± 0.03
6	F6	192.6 ± 3.18	0.291 ± 0.09
7	F7	97.6 ± 1.37	0.137 ± 0.05
8	F8	201.3 ± 3.42	0.238 ± 0.08
9	F9	175.4 ± 1.48	0.109 ± 0.06

Data were expressed as mean ± SD (n=3)

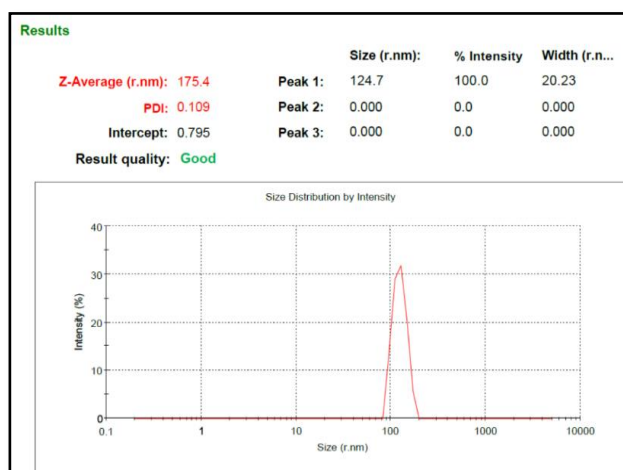


Fig. 2 Particle size and PDI of optimized formulation F9

Determination of zeta potential

The zeta potential of the polymeric nanoparticles is important to determine the stability and uptake mechanism of the particles inside the body. The zeta potential of the formulations F1-F9 is shown in table 5 and zeta potential of optimized formulation F9 is shown in fig. 3.

Table 5 Evaluations of Zeta potential (F1-F9)

Sr. No.	Formulation code	Zeta potential (mV)
1	F1	-6.8 ±0.26
2	F2	-12.4 ±0.41
3	F3	-15.2 ±0.32
4	F4	-14.3 ±0.54
5	F5	-12.7 ±0.37
6	F6	-10.2 ±0.30
7	F7	-9.8 ±0.62
8	F8	-10.5 ±0.29
9	F9	-24.0 ±0.33

Data were expressed as mean ± SD (n=3)

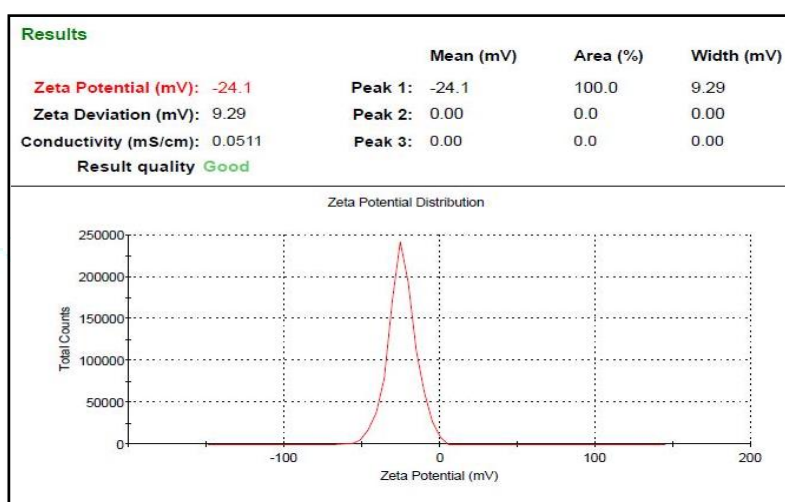


Fig. 3 Zeta potential of optimized formulation F9

Determination of percent entrapment efficiency

The results of percent entrapment efficiency and percent drug loading of formulations F1-F9 are shown in table 6.

Table 6 Formulations of percent entrapment efficiency of formulations F1-F9

Sr. No.	Formulation code	% Entrapment efficiency
1	F1	36 ±3.12
2	F2	33 ±1.95
3	F3	45 ± 3.05
4	F4	43 ±2.68
5	F5	40 ±2.08
6	F6	47 ±1.12
7	F7	31 ±1.98
8	F8	51 ±2.14
9	F9	56 ±3.56

Data were expressed as mean ± SD (n=3)

FT-IR spectroscopy

The FT-IR spectra of VH, PLGA polymer and VH loaded polymeric PLGA nanoparticles (fig. 4 (A), (B), (C) respectively) were recorded from 400-4000 cm⁻¹. The KBr press plate technique was used to prepare sample. The ratio of VH to PLGA polymers was kept at 1:100 for preparation of sample. The FT-IR spectrum of VH shown peaks 1244.11 cm⁻¹ (C-O-C stretching), 1450 cm⁻¹ (-CH₃ bend), 1375 cm⁻¹ (-CH₃ bend), 1465 (-CH₂ bend), 1600 cm⁻¹ (C=C aromatic stretch), 2835.41 cm⁻¹ (cyclic aliphatic -CH stretch), 3328.3 cm⁻¹ (-OH alcohol H-bonded). FT-IR spectrum of PLGA polymer shown the peaks 2358.98 cm⁻¹ (C=O), 1749.47 cm⁻¹ (C=O), 1457.25 cm⁻¹ (C-O), 1273.04 cm⁻¹ (C-C), 2876.88 cm⁻¹ (-CH₃ symmetric), 2946.32 cm⁻¹ (-CH₃ Asymmetric), 3647.45 cm⁻¹ (O-H), 2876.88 cm⁻¹ (C-H symmetric), 2946.32 cm⁻¹ (C-H Asymmetric). The FT-IR spectrum of VH loaded polymeric PLGA NPs shown the peaks 2946.32 cm⁻¹ (C-H asymmetric stretch), 1448.57 cm⁻¹ (-CH₃ bend).

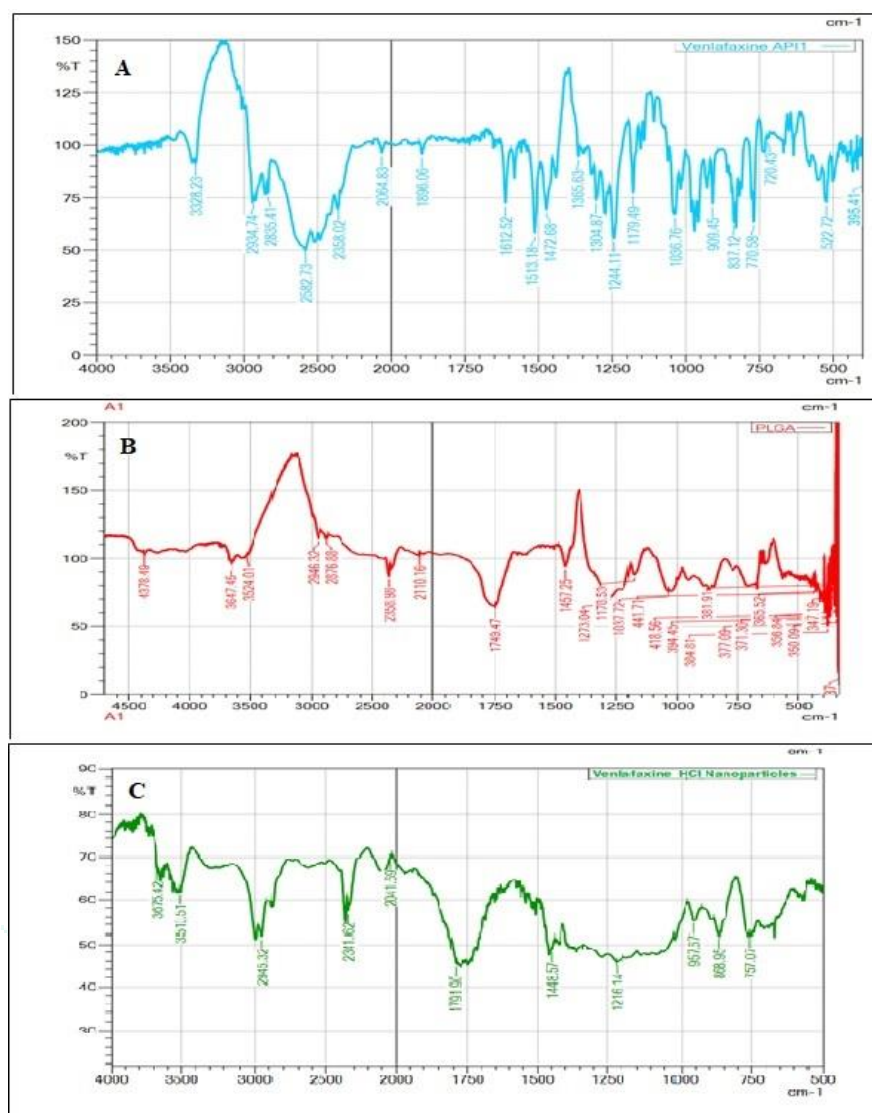
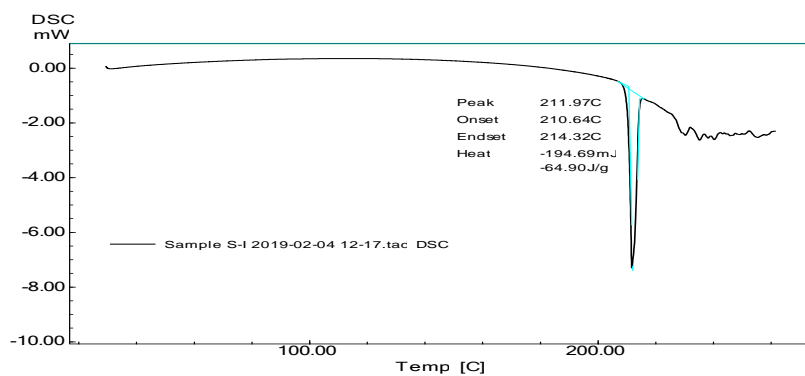


Fig. 4 FT-IR spectrum of VH, PLGA and VH loaded PPNPs(A) FT-IR spectrum of VH (B) FT-IR spectrum of PLGA (C) FT-IR spectrum of VH loaded PPNPs

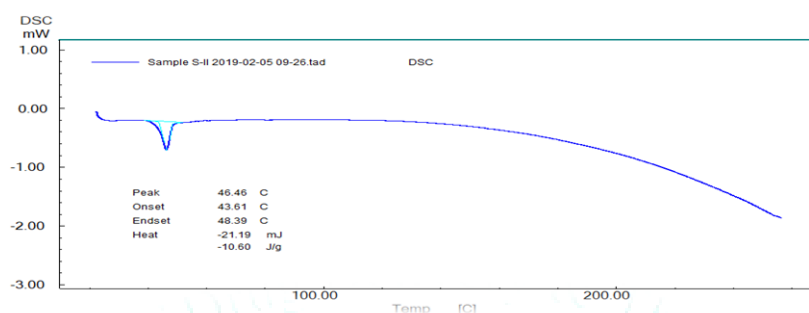
Differential scanning calorimetry

The DSC thermogram of VH, PLGA and VH loaded PPNPs (shown in fig. 5 (A), (B), (C) respectively) were recorded SHIMADZU DSC instrument. The heating rate was kept at 5 °C/min. up to 300 °C. The DSC thermogram of VH shown the onset of melting process at 210.64 °C and endset at 214.32 °C. A sharp melting peak was observed at 211.97 °C which was found to be near to the reported value 215-217 °C as melting point range of VH. The enthalpy for the endothermic transition was found to be (-) 64.90 J/g. PLGA polymer

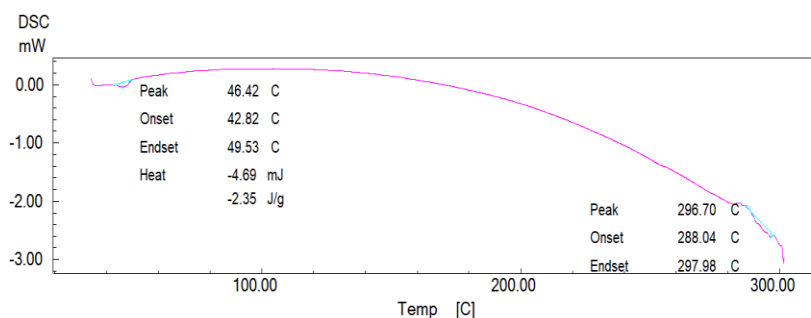
shown the onset of melting point at 43.6 °C and end set at 48.39 °C with glass transition temperature at 46.40 °C which was found to be as per the reported value of glass transition temperature for PLGA at 44-48 °C. The VH loaded PPNPs were subjected to DSC analysis. It showed the onset at 42.21 °C and endset at 46.94 °C with an endothermic peak 44.48 °C which was found to be similar to glass transition temperature of PLGA polymer. The absence of endothermic transition of VH indicated the coating of drug due to formation of polymeric nanoparticles.



A



B



C

Fig. 5 DSC thermogram of VH, PLGA and VH loaded PNPs (A) DSC thermogram of VH (B) DSC thermogram of PLGA (C) DSC thermogram of VH loaded PNPs

X ray diffraction spectroscopy study

The powder x-ray diffraction spectrum of VH, PLGA polymer and VH loaded PLGA nanoparticles were reported at an angle 2θ (Fig. 6). The following sharp peaks with intensities were observed at an angle 2θ at 6.82, 8.15, 10.34, 12.83, 13.62, 15.13, 17.44, 18.35, 19.88, 21.32, 21.85, 22.61, 22.89, 25.19, 26.43, 27.33, 28.68, 31.22, 33.35, 34.14, 35.20, 37.77. The sharp crystalline peaks at an angle 2θ confirmed the crystalline characteristics of VH. In case PLGA polymer the

diffused pattern was observed and no sharp crystalline peak was present in the x-ray diffraction spectra. It indicating amorphous characteristics of the PLGA polymer. VH loaded polymeric PLGA nanoparticles has shown a diffused pattern in the X-RD spectra. It indicating the formation of nanoparticles. The PLGA polymer coat being present on drug molecule, hence the crystalline characteristics of VH was not observed in X-ray diffraction spectrum of polymeric NPs as shown in fig. 6 (A), (B), (C) respectively.

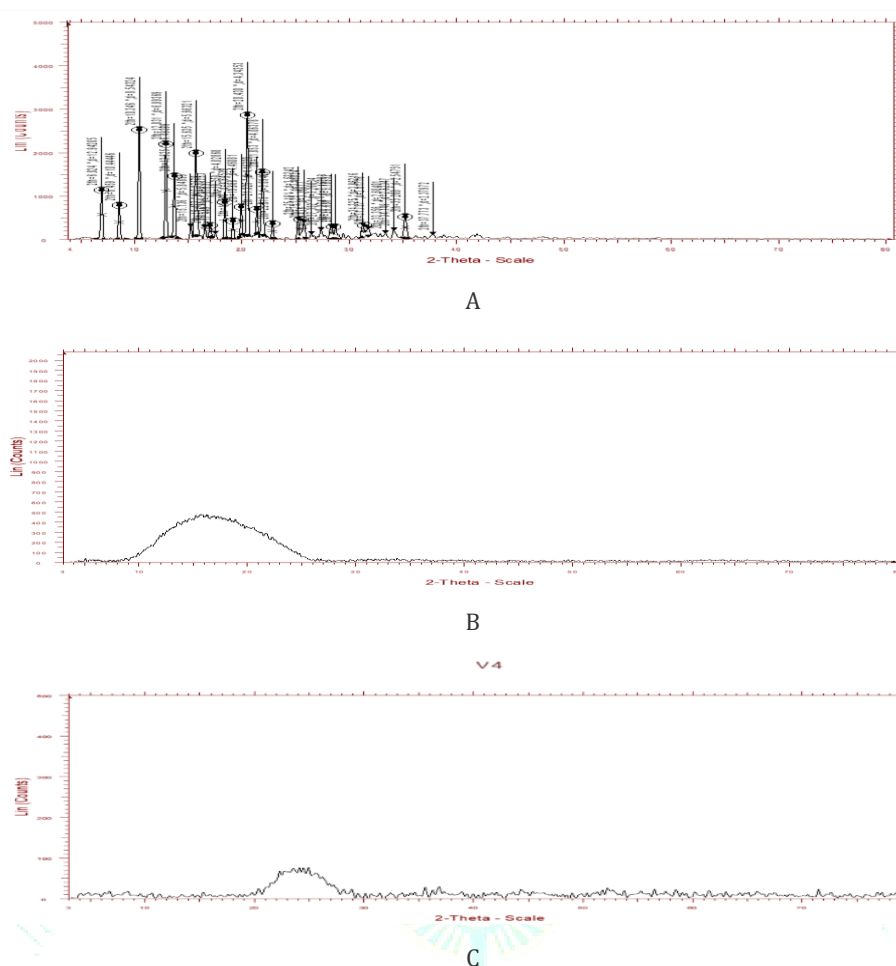


Fig. 6 X-RD spectrum of VH, PLGA and VH loaded PNPs (A) X-RD spectrum of VH (B) X-RD spectrum of PLGA (C) X-RD spectrum of VH loaded PNPs

Surface morphology study

Scanning electron microscopy of lyophilized VH loaded polymeric PLGA nanoparticles is shown in fig 7. A well-formed spherical polymeric nanoparticles containing VH were observed.

Ex-vivo permeation study

The *ex-vivo* permeation study VH was carried using ethanol, propylene glycol and their binary combinations with distilled water in various proportions and penetration enhancers were studied for their effect on skin permeation (Table 7).

Table 7 *Ex-vivo* effect of the solvent systems, permeation enhancers and nanoparticles on lag time, flux, and permeation parameters of VH

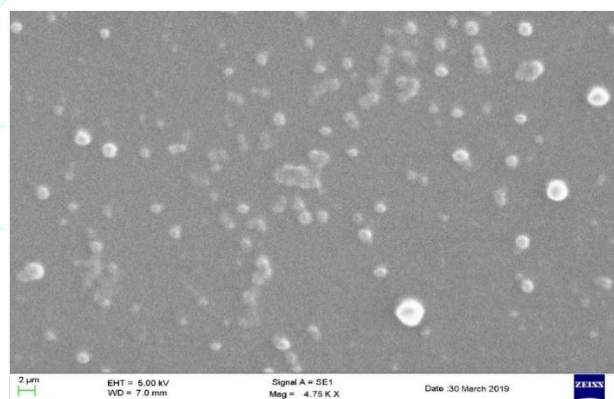


Fig. 7 Scanning electron microscopy study of VH loaded polymeric PLGA nanoparticles

Table 7 Ex-vivo effect of the solvent systems, permeation enhancers and nanoparticles on lag time, flux, and permeation parameters of VH

Sr. No.	FC	SS PE PNPs	Lag time (h.)	Flux ($\mu\text{g}/\text{cm}^2/\text{h}$)	Steady state permeability coefficient (K_p) (cm/h)	Enhancement ratio (ER)
1	W	DW (Control)	6.22 \pm 0.26	79.65 \pm 1.2	2.12	1.0
2	NPs	Nanoparticles	4.22 \pm 0.14	192.24 \pm 3.6	5.12	2.41
3	V1	33% EtOH in DW	5.80 \pm 0.19	114.75 \pm 1.9	3.06	1.44
4	V2	50% EtOH in DW	5.58 \pm 0.15	137.08 \pm 2.7	3.65	1.72
5	V3	66% EtOH in DW	5.49 \pm 0.20	142.30 \pm 2.9	3.79	1.78
6	V4	100 % EtOH	6.00 \pm 0.28	118.29 \pm 2.6	3.15	1.48
7	V5	33% PG in DW	5.86 \pm 0.21	106.41 \pm 2.1	2.83	1.33
8	V6	50% PG in DW	5.73 \pm 0.13	111.69 \pm 2.5	2.97	1.40
9	V7	66% PG in DW	5.62 \pm 0.26	122.78 \pm 2.8	3.27	1.54
10	V8	100% PG	6.12 \pm 0.34	85.82 \pm 1.0	2.28	1.07
11	V9	33% PG in EtOH	5.52 \pm 0.23	150.22 \pm 1.9	4.00	1.88
12	V10	50% PG in EtOH	5.60 \pm 0.16	158.67 \pm 2.9	4.23	1.99
13	V11	66% PG in EtOH	6.00 \pm 0.28	147.05 \pm 2.7	3.92	1.84
14	V12	5% Cineole (50% PG in EtOH)	5.77 \pm 0.17	177.20 \pm 3.4	4.72	2.22
15	V13	5% Limonene (50% PG in EtOH)	3.17 \pm 0.11	200.47 \pm 3.6	5.34	2.51
16	V14	5% Menthol (50% PG in EtOH)	5.90 \pm 0.19	163.52 \pm 2.9	4.36	2.05

Data were expressed as Mean \pm SD (n=3)

FC- Formulation code, SS-solvent system, PE-permeation enhancers, PNPs- polymeric poly (lactic co-glycolic acid), DW- distilled water, PG- propylene glycol, EtOH- Ethanol, Kp- Permeability coefficient, ER-Enhancement ratio

In the *ex-vivo* skin permeation studies of VH using distilled water as solvent system shown the lag time 6.22 h and flux value 79.65 $\mu\text{g}/\text{cm}^2/\text{h}$ was observed and was treated as control. The binary combinations of ethanol 33% to 66% in distilled water has shown decreased lag times (5.80 \pm 0.19, 5.58 \pm 0.15 5.49 \pm 0.20) and the flux values were found to be increased (114.75 \pm 1.9, 137.08 \pm 2.7, 142.30 \pm 2.9). At 100% ethanol, lag time was found to be further enhanced (6.00 \pm 0.28 h) and the flux value was also reduced (118.29 \pm 2.6) as compared to 66% ethanol in distilled water and control. Since VH is water soluble drug, the increasing concentration

of ethanol may have increased the bilayer fluidity which can be explained by the increased in rate and amplitude of translational and rotational motion of individual of -CH group of acyl chain of lipids of stratum corneum. The increased lag time at 100% ethanol concentration may be due to dehydration of skin which results in increased tortuosity of diffusion pathway (Bommanan *et al.*1991). As compared to control, in case of ethanol lag time was found to be higher but was decreased with increasing ethanol concentration up to 66% as shown in fig.8 (A), (B), (C) respectively.

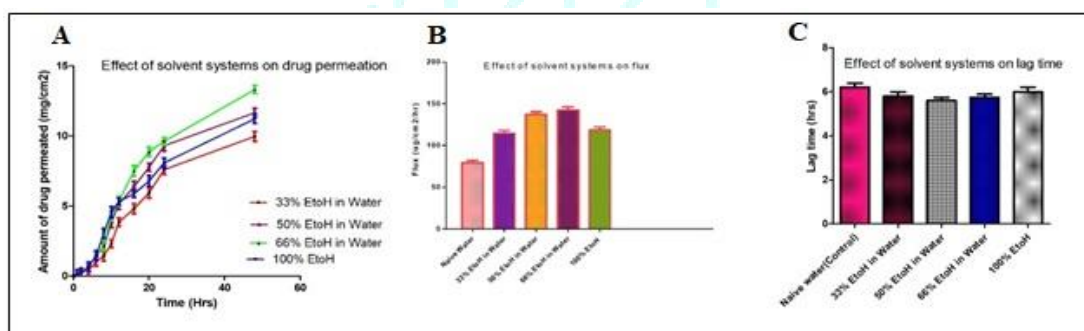


Fig. 8 Effect of solvent system on (A) amount of drug permeation (B) flux (C) lag time (33% - 100% EtOH in DW)

Propylene glycol in distilled water in concentration 33 to 66% shown decreased lag time values (5.86 \pm 0.21, 5.73 \pm 0.13, 5.62 \pm 0.26) and the lag time value was found to be lower than control (6.22 \pm 0.26) and at 100% PG the maximum lag time was observed (6.12 \pm 0.34) (Table 7). Similarly, the flux value was found to increase (106.41 \pm 2.1, 111.69 \pm 2.5, 122.78 \pm 2.8) from 33% to 66% PG in distilled water but the flux was decreased (85.82 \pm 1.0) at 100% PG as shown in Fig.9 (A), (B), (C) respectively. It is due to

hygroscopic nature of PG, since PG forms pools inside skin, thereby leading to dehydration of skin (Ostrenga *et al.* 1971). The pool formation in skin is expected at all concentrations of PG but at 100% PG free water present was negligible to satisfy the hydration requirement of PG. Thus at 100% PG extracts water from skin bilayers and corneocytes pockets and leading to increasing in barrier property of stratum corneum.

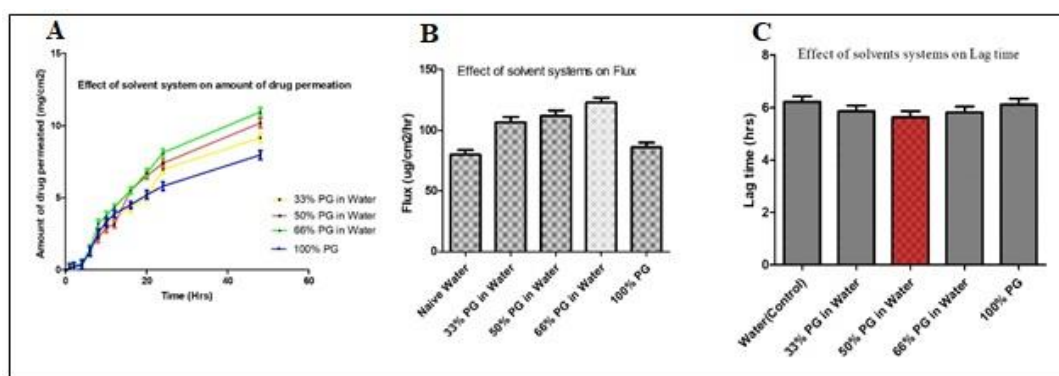


Fig. 9 Effect of solvent system on (A) amount of drug permeation (B) flux (C) lag time (33% to 100% PG in DW)

The lag time in binary combinations of propylene glycol in ethanol in 33, 50, and to 66% were found 5.52 ± 0.23 , 5.60 ± 0.16 , 6.00 ± 0.28 respectively. The lag time was found to increase with increasing concentration of PG in ethanol. The flux value in 33, 50, and to 66% PG in ethanol were found to

be 150.22 ± 1.9 , 158.67 ± 2.9 , 147.05 ± 2.7 $\mu\text{g}/\text{cm}^2/\text{h}$. With the binary combination 33% and 50% PG in ethanol, flux were found to be enhanced but at 66% PG in ethanol the flux was further decreased as shown in fig. 10 (A), (B), (C) respectively.

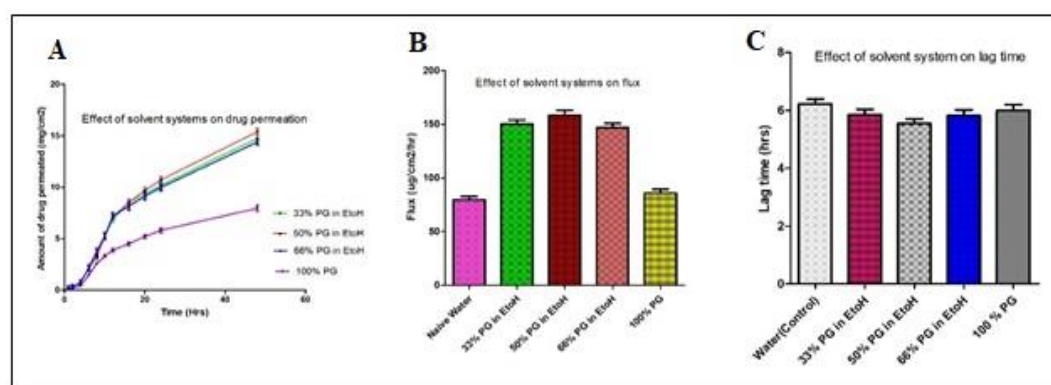


Fig. 10 Effect of solvent system on (A) amount of drug permeation (B) flux (C) lag time (33 -66% PG in EtOH)

d) From above solvent systems, the solvent systems comprising 50% propylene glycol in ethanol shown maximum flux value and minimum lag time as compared to control. Hence the effect of penetration enhancers cineole, limonene, and menthol in 5 % concentrations were studied in the above solvent system. The minimum lag time value

was observed with 5% limonene in 50% PG in ethanol and shown the highest flux (200.47 ± 3.6) than control (79.65 ± 1.2) as shown in Table 7 and fig. 11(A), (B), (C) respectively. Hence, we can conclude that the above solvent system can be used for the transdermal drug delivery of VH.

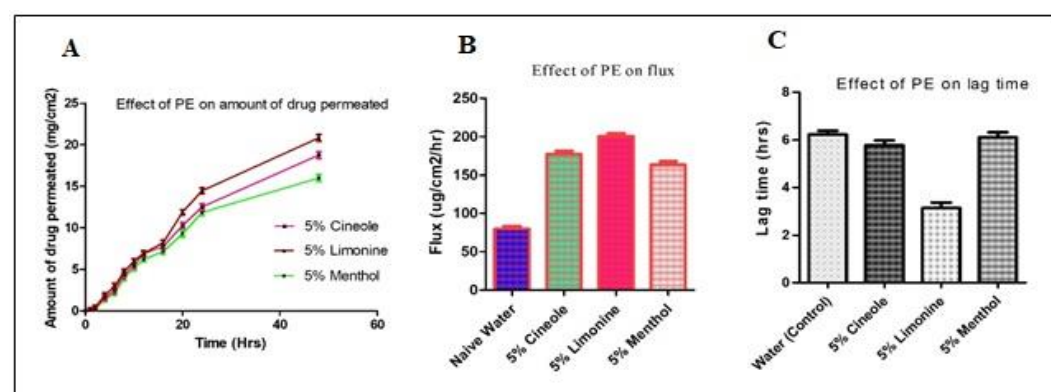


Fig. 11 Effect of permeation enhancers on (A) amount of drug permeation (B) flux (C) lag time (5% PE)

The meaningful plasma level concentrations can be achieved by taking considerations by flux value, clearance value of drug and surface area of transdermal patch.

Pharmacokinetic parameters of VH

CL = 1.3 ± 0.6 liter/hour/kg

$V_d = 7.5 \pm 3.7$ liter/kg

$T_{1/2} = 5 \pm 2$ hours

BA = 42 ± 15 %

$C = (J_a \times S_a) / CL$

Where, C = Steady state plasma Concentration

J_a = Flux

S_a = Surface area

CL = Clearance

The maximum flux achieved was $200.47 \mu\text{g}/\text{cm}^2/\text{hr}$

$C = (J_a \times S_a) / CL$

$$C = \frac{200.47 \mu\text{g}/\text{cm}^2/\text{h} \times S_a [\text{cm}^2]}{78,000 [\text{mL}/\text{h}]}$$

Steady state concentrations of VH from 12.85 ng/mL to 128.5 ng/mL can be obtained with patch size of 5 cm^2 to 50 cm^2 respectively shown in table 8.

Table 8 Steady state concentration of VH

Sr. No.	Surface area of patch (cm^2)	Steady state plasma level of VH (ng/mL)
1	5	12.85
2	10	25.70
3	20	51.40
4	30	77.10
5	40	102.8
6	50	128.5

CONCLUSION

Nanoparticles represent a tool to transport the necessarily drugs across the BBB that normally are unable to cross this barrier. Drug that have successfully have been transported into the brain using this carrier include polymeric poly (lactic co-glycolic acid). Tween-80 was used as surfactant in nanoparticle formulation.

Ex-vivo skin permeation study of VH was carried out in different solvent systems and results indicated that solvent system comprising 50 % PG in ethanol shown maximum flux of $158.67 \pm 2.9 \mu\text{g}/\text{cm}^2/\text{h}$ and lag time 5.60 ± 0.16 h, maximum permeability coefficient $4.23 \text{ cm}/\text{h}$ and maximum enhancement ratio 1.99 was observed as compared to other solvent systems studied.

Ex-vivo skin permeation study of VH was carried out in different PEs and results indicated that 5%v/v limonene shown maximum flux $200.47 \pm 3.6 \mu\text{g}/\text{cm}^2/\text{h}$ and least lag

time of 3.17 ± 0.11 h, maximum permeability coefficient $5.34 \text{ cm}/\text{h}$ and maximum enhancement ratio 2.51 was observed as compared to other PEs. The rank order was observed for skin permeation of VH in different PEs: limonene > cineole > menthol. Limonene was increasing partitioning of a drug into stratum corneum which leads to increased permeation rate of drug.

Ex-vivo skin permeation study of VH -PPNPs was carried out and compared with control group (distilled water) and results indicated that VH -PPNPs shown maximum flux of $192.24 \pm 3.6 \mu\text{g}/\text{cm}^2/\text{h}$ and least lag time 4.22 ± 0.14 h, maximum permeability coefficient $5.12 \text{ cm}/\text{h}$ and maximum enhancement ratio 2.41 was observed as compared to control group (distilled water).

From the above observation, it was concluded that combination of optimized solvent system (50% PG in ethanol), optimized PE (5 %v/v limonene) and VH-PPNPs may be choice for use in a novel transdermal formulation of VH.

Based on the clearance value of VH ($78000 \text{ mL}/\text{h}$), maximum flux value obtained $200.47 \pm 2.54 \mu\text{g}/\text{cm}^2/\text{h}$ and by varying the surface area of the transdermal patch from 5 cm^2 to 50 cm^2 , a meaningful plasma level concentration of VH ranging from 12.85 to 128.5 ng/mL can be achieved.

REFERENCES

- Abbott N., Patabendige A., Dolman D., Yusof S., Begley D. (2010) Structure and function of the blood-brain barrier, *Neurobiology of Disease* 37, 13-25, DOI: 10.1016/j.nbd.2009.07.030
- Acharya S. and Sahoo S., (2011) PLGA nanoparticles containing various anticancer agents and tumour delivery by EPR effect, *Advanced Drug Delivery Reviews* 63, 170-183, DOI: 10.1016/j.addr.2010.10.008
- Alexis F, Pridgen E, Molnar LK, Farokhzad OC (2008) Factors affecting the clearance and biodistribution of polymeric nanoparticles. *Mol Pharm* 5(4):505-515. DOI:10.1021/mp800051m
- Anderson J. and Shive M. (1977) Biodegradation and biocompatibility of PLA and PLGA microspheres. *Advanced Drug Delivery Reviews*, 28(1):5-24. PMID:10837562
- Barch D., (2013) Introduction to Special Issue on the Neurobiology of Depression, *Neurobiology of Disease* 52, 1-3 DOI.org/10.1016/j.nbd.2012.10.026
- Bellavance M., Blanchette M and Fortin D., (2008) Recent Advances in Blood-Brain Barrier Disruption as a CNS Delivery Strategy, *The AAPS Journal*, 10(1):166-177, DOI: 10.1208/s12248-008-9018-7
- Bilati U., Alle E. and Doelker E. (2005) Poly (D,L-lactide-co-glycolide) protein-loaded nanoparticles prepared by the double emulsion method—processing and formulation issues for enhanced entrapment efficiency, *Journal of Microencapsulation*, 22(2): 205-214, DOI: 10.1080/02652040400026442
- Bommannan. D., Russell P., and Guy R. (1991) Examination of the effect of ethanol on human stratum corneum *in-vivo* using infrared spectroscopy, *Journal of Controlled Release*, 16 299-304, PMID:5127090
- Danhier F., Ansorena E., Silva J., Coco R., Breton A., Preat V., (2012) PLGA-based nanoparticles: An overview of biomedical applications, *Journal of Controlled Release* 161:505-522, DOI:10.1016/j.jconrel.2012.01.043
- Dinas P., Koutedakis Y., Flouris Y., (2011) Effects of exercise and physical activity on depression, *Ir J Med Sci* 180:319-325, DOI 10.1007/s11845-010-0633-9
- Gohel M., and Bariya S., (2009) Advanced formulation design of VH coated and triple-layer tablets containing Hypromellose, *Pharmaceutical Development and Technology*, 14(6): 650-658, DOI: 10.3109/10837450902911911
- Gulati N., Nagaich U, Saraf S,(2014) Fabrication and *in-vitro* characterization of polymeric nanoparticles for Parkinson's therapy: a novel approach, *Brazilian Journal of Pharmaceutical*

- Sciences, vol. 50(4) DOI.org/10.1590/S1984-82502014000400022
13. Katara R., Sachdeva S., and Majumdar D., (2017) Enhancement of ocular efficacy of aceclofenac using biodegradable PLGA nanoparticles: formulation and characterization, Drug Deliv. and Transl. Res. DOI:10.1007/s13346-017-04161
 14. Krishnaiah Y., and Al-Saidan S., (2008) Limonene Enhances the *In-Vitro* and *In-Vivo* Permeation of Trimetazidine Across a Membrane-Controlled Transdermal Therapeutic System, Current Drug Delivery, 5, 70-76, PMID:18220554
 15. Lopez E., Ettcheto M., Egea1 M., Espina M., Cano A., Calpena A., Camins A., Carmona N, Silva A., Souto E.
 16. and García M., (2018) Memantine loaded PLGA PEGylated nanoparticles for Alzheimer's disease: *in-vitro* and *in-vivo* characterization, J Nanobiotechnology, 16:32 <https://doi.org/10.1186/s12951-018-0356-z>
 17. Narishetty R., Sunil T., (2005) Effect of l-menthol and 1,8-cineole on phase behavior and molecular organization of SC lipids and skin permeation of zidovudine. J. Control. Release 102, 59-70 DOI:10.1016/j.jconrel.2004.09.016
 18. Ng K, Xiong S, Zhao X, Heng B, Loo J, (2011) Cellular uptake of poly-(D,L-lactide-co-glycolide) (PLGA) nanoparticles synthesized through solvent emulsion evaporation and nanoprecipitation method, Biotechnol. J. 6, 501-508 DOI 10.1002/biot.201000351
 19. Ostrenga J., Steinmetz C., Poulsen B., (1971) Significance of Vehicle Composition I: Relationship between Topical Vehicle Composition, Skin Penetrability, and Clinical Efficacy, Journal of Pharmaceutical sciences, 60(8);1175-1179. DOI :<https://doi.org/10.1002/jps.2600600812>
 20. Panchagnula R., Salve P., Thomas N., Jain A., Poduri R., (2001) Transdermal delivery of naloxone: effect of water, propylene glycol, ethanol and their binary combinations on permeation through rat skin, International Journal of Pharmaceutics 219, 95-105 PMID:11337170
 21. Panchagnula R., Bokali R., Sharma P., Khandavilli S., (2005) Transdermal delivery of naloxone: skin permeation, pharmacokinetic, irritancy and stability studies, International Journal of Pharmaceutics 293, 213-223, DOI:10.1016/j.ijpharm.2005.01.004
 22. Patel H., Shah S., Shah D., Joshi P., (2011) Sustained release of venlafaxine from venlafaxine-montmorillonite-polyvinylpyrrolidone composites. Appl. Clay Sci., 51, 126-130 DOI org/10.1016/j.clay.2010.11.013
 23. Rao J., (2011) Geckeler K., Polymer nanoparticles: Preparation techniques and size-control
 24. Parameters, Progress in Polymer Science 36 (2011) 887-913, DOI 10.1016/j.progpolymsci.2011.01.001
 25. Sawant K., Seju U., Kumar A., (2011) Development and evaluation of olanzapine-loaded PLGA nanoparticles for nose-to-brain delivery: *In-vitro* and *in-vivo* studies, Acta Biomaterialia 7 (2011) 4169-4176, DOI:10.1016/j.actbio.2011.07.025
 26. Shah D., Khandavilli S. and Panchagnula R., (2008) Alteration of Skin Hydration and its Barrier Function by Vehicle and Permeation Enhancers: A Study using TGA, FTIR, TEWL and Drug Permeation as Markers, Methods Find Exp Clin Pharmacol, 30(7): 499-512 DOI: 10.1358/mf.2008.30.7.1159653
 27. Tosi G, Costantino L, Ruozzi B, Forni F, Vandelli A., (2008) Polymeric nanoparticles for the drug delivery to the central nervous system. Expert Opin. Drug Deliv. 5, 155-174 PMID:23458620
 28. Tripathi K. D., (2009) Essentials of Medical Pharmacology, 6th Edition, Jaypee Brothers Publishing House Pvt. Ltd. Reprint;476-556.
 29. Vandervoort J, Ludwig A, (2002) Biocompatible stabilizers in the preparation of PLGA nanoparticles: a factorial design study, International Journal of Pharmaceutics 238,77-92 DOI org/10.1016/S0378-5173(02)00058-3
 30. Yang Z., Teng, Y., Wang H., Hou H., (2013) Enhancement of skin permeation of bufalin by limonene via reservoir type transdermal patch: Formulation design and biopharmaceutical evaluation. Int. J. Pharm., 447, 231-240 DOI:10.1016/j.ijpharm.2013.02.048
 31. Zhou Y, Zhang G, Rao Z, Yang Y, Zhou Q, Qin H, Wei Y, Wu X, (2015) Increased brain uptake of venlafaxine loaded solid lipid nanoparticles by overcoming the efflux function and expression of P-gp Arch. Pharm. Res. 38:1325-1335 DOI 10.1007/s12272-014-0539-6

